Comparison of Raman lidar and GPS measurements at the COPS Vosges supersite

Pierre Bosser[1], Olivier Bock[2], Cédric Champollion[3]

(1) LOEMI / IGN, Saint-Mandé, France, Pierre.Bosser@ign.fr - (2) LAREG / IGN, Marne-La-Vallée, France - (3) GM / CNRS, Montpellier, France

Context

A

Institut Géographique National (IGN, France) and Service d'Aéronomie (SA, France) have conjointly developed a mobile Raman lidar system [Tarniewicz et al., 2002]. IGN-SA lidar is intended to be used in close relation with GPS measurements for two specific applications: the study of water vapor heterogeneity in lower troposphere and the calibration of GPS measurements for high accuracy GPS positioning [Bock et al., 2001].

IGN-SA Raman lidar has been operating during the whole month of July 2007 at the COPS Vosges supersite, for about 200 h in 25 measurement sessions. It was first intended to work for nighttime and daytime sessions. However, due the difficulty to perform accurate water-vapor measurements during daytime sessions, nighttime and transitional periods observations were favored

Lidar water vapor mixing ratio profiles

B

Lidar water vapor mixing ratio profiles are calibrated using nighttime collocated radiosoundings from 4M (CNRM - Météo-France) on the range 1-3 km (10 calibration sessions). More details about the retrieval algorithms can be found in [Bosser et al., 2007].

The agreement between water-vapor mixing ratio profiles retrieved by lidar and collocated radiosoundings up to maximum range are rather good with a very similar sensing of the different inversion layers.

The evolution of the mixing ratio profiles observed by lidar gives an interesting view into the evolution of the nocturnal atmospheric boundary layer and the day / night transitions. This product can be important additional information source to numercal weather prediction models for water-vapor evolution studies.

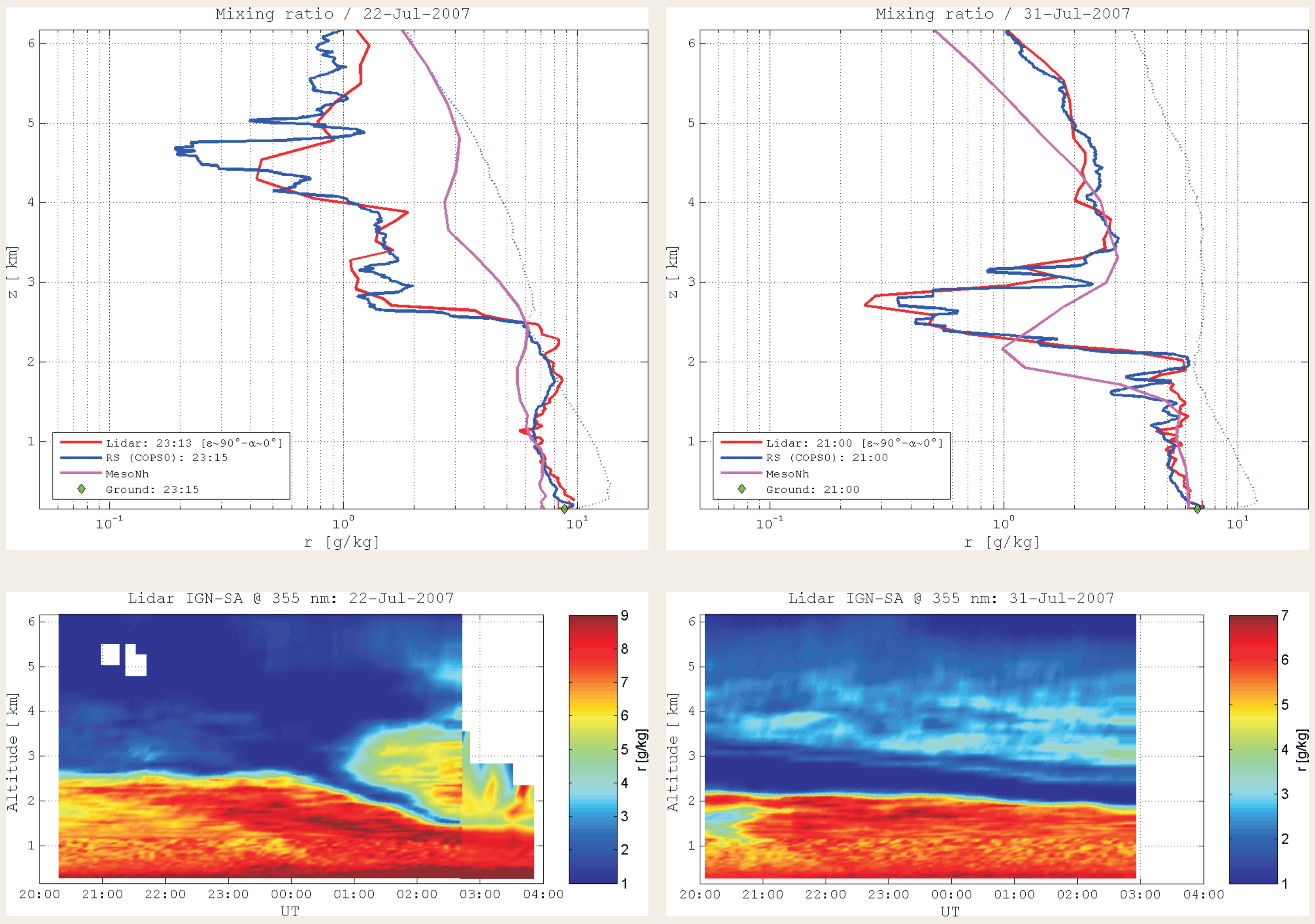

FIG 1: Water vapor mixing ratio retrieval during 22[th] and 31[st] of July lidar sessions. Up : comparison of water vapor mixing ratio profiles from lidar, radiosonde (RS92 from 4M / CNRM) and Meso-nh (Meso-nh data: courtesy E. Richard, LA / CNRS). Bottom : lidar water vapor mixing ratio profiles evolution.

GPS processing

C

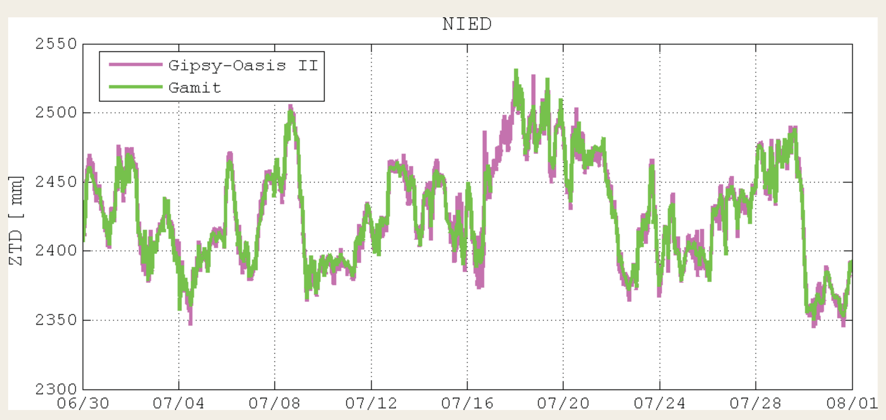

FIG 2: Evolution of tropospheric delays from Gipsy-Oasis II and Gamit processing.

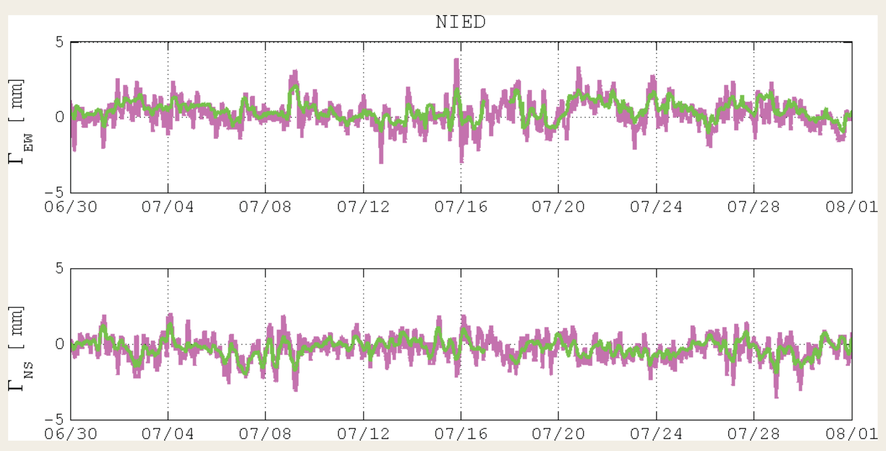

FIG 3: Evolution of horizontal gradients from Gipsy-Oasis II and Gamit processing.

GPS data are processed using 2 different GPS processing software

- Gipsy-Oasis II (v. 5.0) : PPP processing for NIED GPS station located on COPS Vosges supersite. Tropospheric delays and horizontal gradients are estimated every 5 minutes.

- Gamit (v. 10.3) : Network processing from COPS GPS network, including NIED GPS station. Tropospheric delays and horizontal gradients are estimated every hour.

Data for NIED station are available over one month (from 29[th] of June to 1[st] of August). GPS processing use the more recent models for troposphere correction (VMF, [Boehm et al., 2006]) and absolute model for GPS antenna calibration.

w.r.t. Gamit	n_{obs}	*b* [mm]	σ [mm]	*r*
G_{EW}	758	0.2	0.6	0.79
G_{NS}	758	0.1	0.5	0.77
ZTD	758	0.6	5.3	0.99

TAB I: Comparison of GPS tropospheric solutions (horizontal gradients and tropospheric delays): bias, standard deviation and correlation.

Integrated water vapor measurements

D

Integrated water vapor measurements are calculated for each instruments.

- Lidar: Water vapor mixing ratio profiles are completed by a close radiosounding profile above 6 km and are integrated up to 15 km.

- GPS: Integrated water vapor values are retrieved using tropospheric delay estimates from GPS processing and pressure and temperature ground measurements [Bosser at al., 2007].

- Radiosonde (RS92) and Meso-nh: Water vapor profiles are integrated up to 15 km to retrieve integrated water vapor contents.

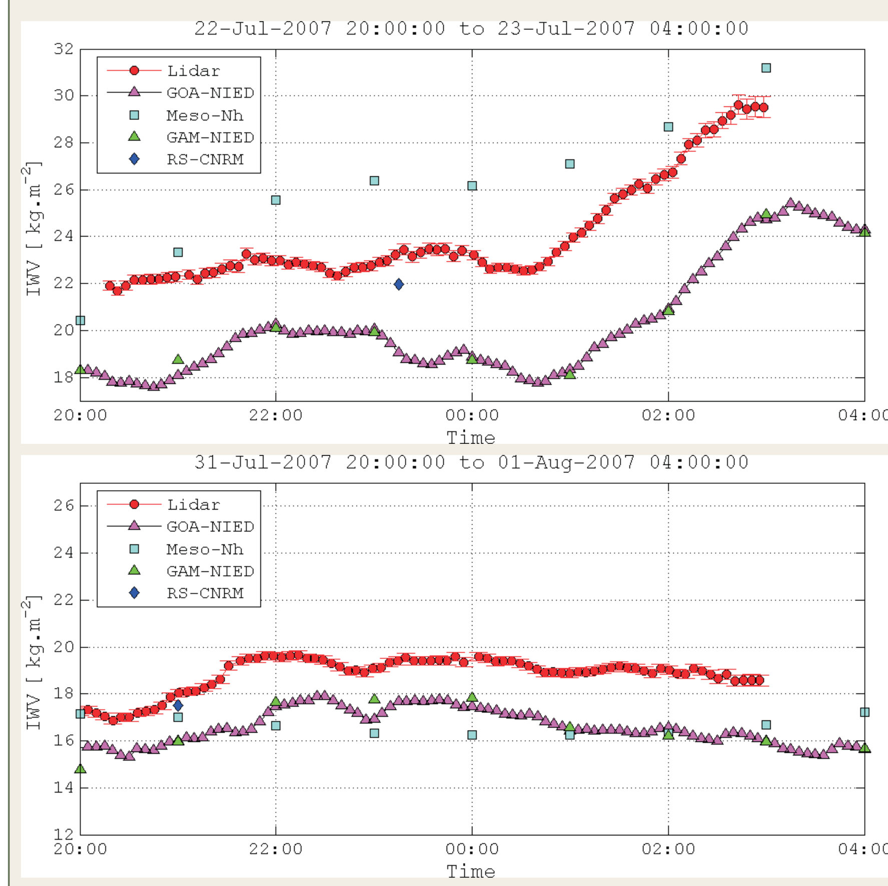

FIG 4: Evolution of integrated water vapor contents from lidar, GPS processing (Gamit and Gipsy-Oasis II), Meso_nh and radiosonde during 22[th] and 31[st] of July lidar sessions.

w.r.t. Radiosonde	n_{obs}	*b* [kg·m^{-2}]	σ [kg·m^{-2}]
Lidar	13	0,2	0,8
Meso-nh	96	-1,3	5,7
GPS – Gamit	95	-1,4	1,3
GPS – Gamit (D)	66	-1,2	1,4
GPS – Gamit (N)	29	-1,9	0,9
GPS – Gipsy	101	-1,5	1,4
GPS – Gipsy (D)	67	-1,2	1,5
GPS – Gipsy (N)	34	-2,0	1,0

w.r.t. Lidar	n_{obs}	*b* [kg·m^{-2}]	σ [kg·m^{-2}]	*r*
Meso-nh	86	-1,8	3,8	0,84
GPS – Gamit	86	-3,1	2,1	0,70
GPS – Gipsy	873	-3,0	1,5	0,49

w.r.t. Meso-nh	n_{obs}	*b* [kg·m^{-2}]	σ [kg·m^{-2}]	*r*
GPS – Gamit	709	-0,4	4,8	0,67
GPS – Gipsy	733	-0,4	4,9	0,69

TAB 2: Comparison of integrated water vapor contents from lidar, GPS processing (Gamit and Gipsy-Oasis II), Meso_nh and radiosonde during the whole campaign: bias, standard deviation and correlation

Differences between lidar and radiosondes are non-biased with a low variability. However we observe a strong GPS dry bias with respect to radiosondes and lidar. Note that dry bias between radiosonde and GPS is more important for nighttime measurements than for daytime measurements, which appears consistent with [Vömel et al., 2006] (presence of a dry bias during daytime measurements using a RS92 humidity sensor). The radiosonde bias could be confirmed with Meso-nh simulations but variability is high.

GPS and Meso-nh estimates present a lower bias (0,4 kg·m^{-2}) but standard deviations reach important values.

Bias investigation

E

Different sources of discrepancy have been investigated.

(1) GPS antenna models: Previous calibration antenna model were suspected to induce significant errors on GPS solution. However, current used models (absolute calibration) are intended to correct these errors

(2) Spatial drift of radiosondes: We observe systematical drift of balloons towards East direction (FIG. 5). This drift could induce deviation on IWV retrieval. However, the impact on IWV will be lower than the differences previously observed since significant drift is only observed in layers which contribution in IWV is low (for example, from height about 5 km this contribution is inferior to 0.8 kg·m^{-2}).

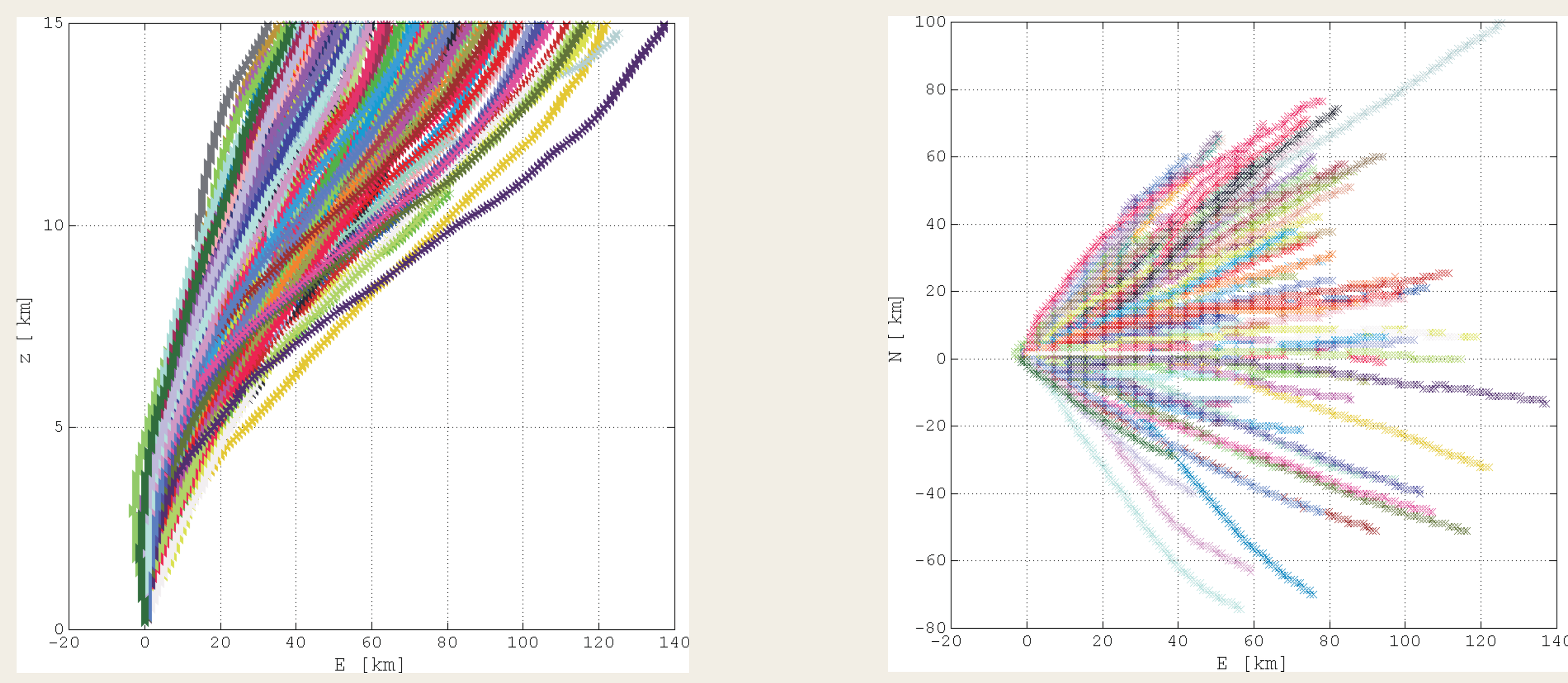

FIG 5: Spatial drift of radiosondes. Left, longitudinal drift in function of latitude. Right, longitudinal drift in function of latitude.

(3) Calibration of radiosondes: The last listed cause of deviation consists in the calibration of the RS92 humidity sensor on balloon. Such error would have a direct impact on lidar retrieval due to the lidar calibration process. However, humidity profiles on FIG 1 show the consistency between lidar, radiosonde and ground measurements. In future investigations, more information would be deduced from airborne lidar water-vapor measurements

Conclusion

F

We have not currently identified the cause of the bias between lidar, radiosonde and GPS solutions. More investigations have to be lead to explain such discrepancies. However, we obtain a good agreement in term of variability (about 1.5 kg·m^{-2}).

In future work, we plan to use the lidar measurements coupling with a ray-tracing algorithm for calibrating the GPS signal for tropospheric delays to demonstrate the capability to achieve mm-level vertical positioning. Such applications has already be lead in previous study and would now be validate thanks to COPS data.

References

Bock, O.; Tarniewicz, J.; Thom, C.; Pelon, J. & Kasser, M., *Study of external path delay correction techniques for high accuracy height determination with GPS*, Physics and Chemistry of the Earth, **26**, 165-171 (2001).

Boehm, J.; Werl, B. & Schuh, H., *Troposphere mapping functions for GPS and very long baseline interferometry from European Centre for Medium-Range Weather Forecasts operational analysis data*, Journal of Geophysical Research, **11**, 2406-+ (2006).

Bosser, P.; Bock, O.; Pelon, J. & Thom, C., *An improved mean gravity model for GPS hydrostatic delay calibration*, Geoscience and Remote Sensing Letters, **4**, 3-7 (2007).

Bosser, P.; Bock, O.; Thom, C. & Pelon, J., *Study of the statistics of water vapor mixing ratio determined from Raman lidar measurements*, Applied Optics, **46**, 8170-8180 (2007).

Tarniewicz, J.; Bock, O.; Pelon, J. & Thom, C., *Raman lidar for external GPS path delay calibration devoted to high accuracy height determination*, Physics and Chemistry of the Earth, **27**, 329-333 (2002).

Vömel, H.; Selkirk, H.; Miloshevich, L.; Valverde-Canossa, J.; Valdès, J.; Kyrö, E.; Kivi, R.; Stolz, W.; Peng, G. & Diaz, J., *Radiation dry bias of the Vaisala RS92 humidity sensor*, Journal of Atmospheric and Oceanic Technology, **6**, 953-963 (2007).